Geotechnical Aspects of Underground Construction in Soft Ground – Viggiani (ed)
© 2012 Taylor & Francis Group, London, ISBN 978-0-415-68367-8

3D Numerical modelling of tunnelling intersecting piles

S.W. Lee, C.K.M. Choy & S.C. Tse
Geotechnical Consulting Group (Asia) Ltd, Hong Kong

F.R. van Gool, W.W.L. Cheang & R.B.J. Brinkgreve
Plaxis BV, Delft University of Technology, The Netherlands

ABSTRACT: Tunnelling beneath existing buildings supported by large numbers of piles is a three-dimensional (3D) soil-structure interaction problem. 3D finite element analyses (FEA) have been carried out to model construction of a 6 m diameter tunnel intersecting the lower portion of a building piled foundation system comprising 50 nos. of 0.6 m diameter, 21.5 m long friction piles. A total of 15 obstructing pile toes are cut off. A step-by-step pressure method is used to model the progressive advance of tunnelling. Two parametric study analyses are carried out to investigate the effects of the upper half of and a full 3 m thick grouted annulus around the tunnel. Results are presented for the responses of selected piles and building settlements. Both grouting schemes are found to be effective in reducing tunnelling-induced ground movements.

1 INTRODUCTION

Tunnelling in densely built-up urban areas often encounters obstructions such as buried utilities/services and existing pile foundations. In some cases the proposed tunnelling alignments were diverted to minimise any potential effect of tunnelling on existing structures. Due to reasons of construction costs, engineering challenges and land resumption, there were cases in which the diversion of tunnel alignments was not feasible, resulting in the tunnels intersecting the toes of existing piles (GCO 1985). In this scenario, the obstructing pile toes were cut off as the tunnel boring machine (TBM) passed through. Protective measures in the forms of superstructure strengthening and grouting beneath the building/around the tunnel were typically carried out prior to tunnelling. The process of pile-cutting was normally carried out manually with temporary stoppage of TBM operation (Pang 2006).

There are limited case histories reporting on the responses of cut piles due to tunnelling, mainly because of the difficulty associated with installing strain gauges in existing piles. This motivates the Authors to carry out 3D finite element analyses (FEA) to investigate the behaviour of piles in a large pile group and associated building in response to tunnelling involving pile-cutting. Parametric studies are carried out to investigate the effectiveness of grouting around the tunnel in mitigating pile/building movements.

2 BACKGROUND INFORMATION

Figure 1 shows the tunnelling problem investigated in this paper. A 6 m diameter bored tunnel will be constructed using a slurry shield Tunnel Boring Machine (TBM) passing through the lower portion of a 10×5 pile group supporting a 23-storey high-rise building. The tunnel axis level is –23 metres Principal Datum (mPD). The segmental tunnel linings are 0.25 m thick. The geometry of the reinforced concrete frame structure building is 17.8 m wide $\times$ 8.8 m long $\times$ 70 m high, orientated perpendicularly to the tunnel alignment. The pile cap geometry is 17.8 m $\times$ 8.8 m $\times$ 1.5 m thick. The piled foundation system comprises 50 nos. of 0.6 m diameter (d) Franki piles, spaced at 3d c/c. The Franki pile is a cast-in-situ concrete pile with an enlarged base and a cylindrical shaft. The pile head and toe levels are –1.5 and –23 mPD respectively. In plan view, 15 nos. of obstructing pile toes are cut off as they intersect the tunnel. The pile toes in Column 2 and Column 1/3 are cut to a level of –19.7 mPD and –20.3 respectively, i.e. 0.3 m above the tunnel extrados.

The ground conditions comprise a 1.5 m thick sandy Fill layer, a 38.5 m thick sandy Completely

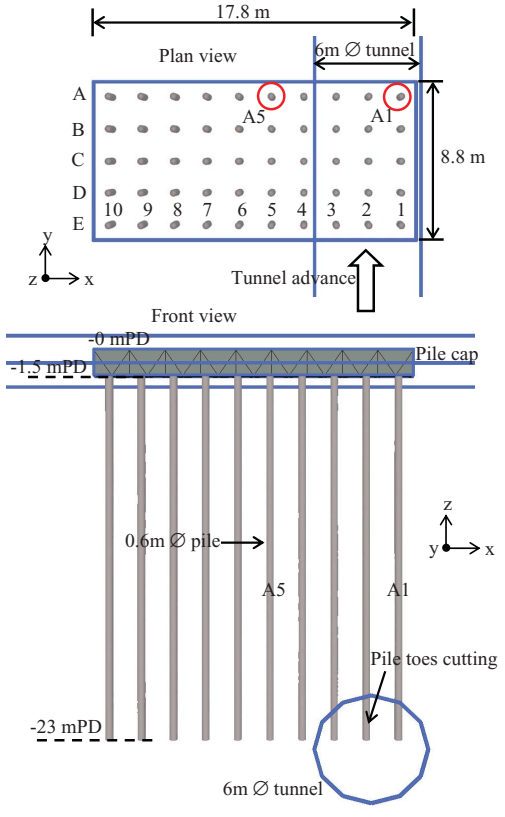

Figure 1. Investigated tunnelling problem.

Decomposed Granite (CDG) layer and bedrock. The ground surface and groundwater levels are 0 mPD and –1.5 mPD respectively.

3 DETAILS OF FEA

The tunnelling problem is analysed using a new commercial 3D FEA programme, Plaxis 3D 2010. Figure 2 shows the 3D model with the mesh refined around the tunnel and in the piled building area. The model geometry is 150 m wide × 120 m long × 40 m high, comprising 79,404 nos. of 10-noded tetrahedral elements. The top of the bedrock corresponds to the bottom boundary of the 3D model.

The non-linear stiffness of the CDG from very small strains ($\varepsilon = 1 \times 10^{-5}\%$) to engineering strain level ($\varepsilon = 1 \times 10^{-2}\%$ to 1%) is modelled using the Plaxis Hardening Soil-Small Strain Stiffness (HSsmall) constitutive model (Benz et al. 2009). The input parameters were calibrated by Lee et al. (2008) against Ng et al.'s (2000) triaxial results on CDG samples carried out at a mean effective stress

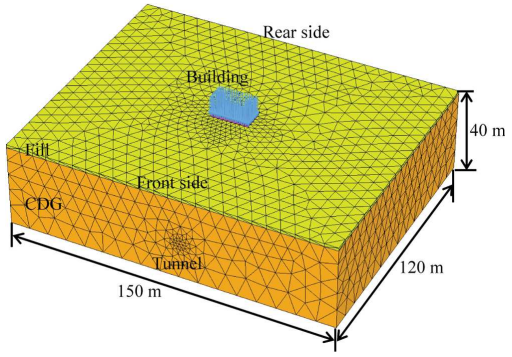

Figure 2. 3D FE model.

Table 1. Soil input parameters.

Parameters*	Fill	CDG
Soil model	HS	HSsmall
Material type	Drained	Drained
γ (kN/m^3)	19	20
E_{50}^{ref} & E_{oed}^{ref} (MPa)	20	39
E_{ur}^{ref} (MPa)	60	117
m [–]	0.5	0.5
c' (kPa)	0.1	5
ϕ' (Deg)	30	35
ν_{ur} [–]	0.2	0.2
p^{ref} (kPa)	100	200
K_0^{nc} [–]	0.5	0.43
G_0^{ref} (MPa)	-	200
$\gamma_{0.7}$ [–]	-	$5(10^{-5}$

* γ = unit weight, $E_{50}^{ref}/E_{oed}^{ref}/E_{ur}^{ref}$ = reference secant/tangent/unloading-reloading stiffness, m = power for stress-dependent stiffness, c' = effective cohesion, ϕ' = effective friction angle, ν_{ur} = Poisson's ratio for unloading-reloading, p^{ref} = reference stress for stiffness, K_0^{nc} = coefficient of earth pressure for normal consolidation, G_0^{ref} = reference shear modulus at very small strains, $\gamma_{0.7}$ = shear strain at $G = 0.722G_0$.

of 200 kPa. The Fill layer is modelled using the Plaxis Hardening Soil (HS) model, which considers the degradation of soil stiffness from a strain level of $1 \times 10^{-2}\%$. Table 1 presents the input parameters for the Fill and CDG.

The pile cap is modelled using linear elastic solid (or volume) elements with a Young's modulus (E) of 20 GPa and a Poisson's ratio (ν) of 0.15. A building loading of 350 kPa (or 47.6 MN) is applied on the top of the pile cap.

The piles are modelled using "Embedded Pile" structural elements. The embedded pile is a slender beam element connected to the surrounding soil by embedded skin (or shaft) and foot (or toe) interfaces (Engin et al. 2008). The pile diameter is input as 0.6 m with an E of 20 GPa, The pile heads are mod-

elled as pinned connections. The enlarged Franki pile base is not modelled. Break points are specified at the pile cutting levels of -19.7 and 20.3 mPD, and the process of pile toe-cutting is modelled by deactivating the pile sections below the two levels.

Potts & Addenbrooke (1997) proposed that the superstructure flexural rigidity (EI) could be estimated using either the Parallel Axis Theorem (i.e. bending about the building neutral axis) or the sum of EI for individual building storeys. The latter is adopted in the 3D analysis, where the superstructure rigidity is modelled using a "Plate" structural element located on the top of the pile cap with a conservative input EI of 3.1×10^8 kNm^2/m and an EA (axial rigidity) of 7.2×10^7 kN/m.

"Plate" structural elements are also used to model the tunnel linings with an input E of 30 GPa and a lining thickness of 0.25 m.

A step-by-step pressure method is used to model the progressive advance of tunnelling. For bored tunnelling in sandy soils, tunnelling contractors will usually apply a tunnel confinement (or face support) pressure defined as: confinement pressure = hydrostatic pore water pressure (pwp) + overpressure. Figure 3 shows the profiles of slurry pressure applied on the tunnel face and grout pressure applied along and around the TBM shield. For a hydrostatic pwp of 185 kPa at the tunnel crown, the modelled face pressures correspond to an overpressure of 20 kPa. The modelled linear varying pressure profile along the shield is to consider the conical shield where its diameter is slightly larger in the front than at the rear, over-cutting and relatively large volume loss into the tail void occurring at the rear of the shield. The pressure profiles could be varied to study the effect of varying the slurry/grouting pressure. It is noted that the shield itself is not modelled in the analysis.

For each advance of the tunnel face, the support pressures shown in Figure 3 are shifted forward by a lining ring width of 1.5 m and correspondingly, a new ring is erected behind the shield. This process is repeated as tunnelling progresses.

In total, three 3D analyses have been carried out as summarised in Table 2.

Analysis 1 is the baseline analysis with no grouting. Analysis 2 investigates the effect of the upper half of a 3 m thick grouted annulus around the tunnel over a horizontal distance of 12 m on reducing tunnelling-induced ground movements, see Figure 4a. The grout is modelled as a linear elastic, perfectly plastic Mohr Coulomb material with an E of 150 MPa, effective cohesion (c') of 100 kPa and effective friction angle (ϕ') of 35°. Analysis 3 models a full 3 m thick grouted annulus, see Figure 4b. Other modelling details for the three analyses remain the same.

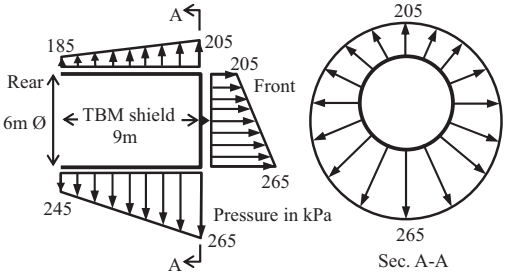

Figure 3. Modelled tunnel support pressures.

Table 2. Details of 3D analyses.

Analyses	Grout
1	No
2	Upper Half of 3 m thick annulus grout
3	Full 3 m thick annulus grout

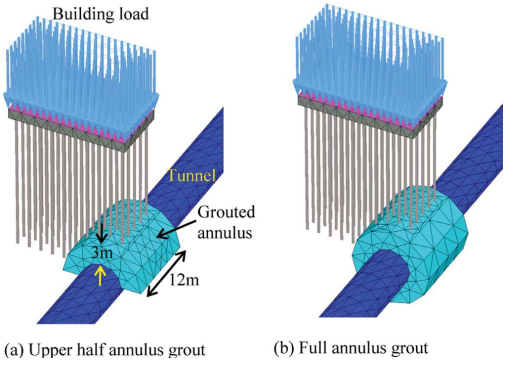

Figure 4. Parametric analyses on grouting effectiveness.

4 RESULTS OF 3D ANALYSES

Figure 5 shows the predicted deformations of the pile group when the tunnel face is well past the rear edge of the pile cap by 53 m for the baseline Analysis 1. The piles settle and displace horizontally towards the tunnel.

Due to space limitations, only results for the most critical pile A1 will be discussed in detail. In general, the A row of piles located in the rear edge of the pile cap show higher pile displacements/stresses. Figure 6 shows the tunnelling stages selected for presentation of results, which correspond to the tunnel face positions at 13 m, 7 m, 1 m before reaching the row A piles (denoted as –13 m, –7 m and –1 m respectively) and at 2 m, 53 m passing beyond the row A piles (denoted as +2 m and +53 m respectively).

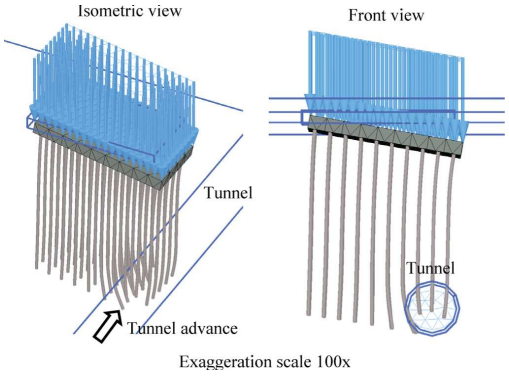

Figure 5. Predicted pile group deformations.

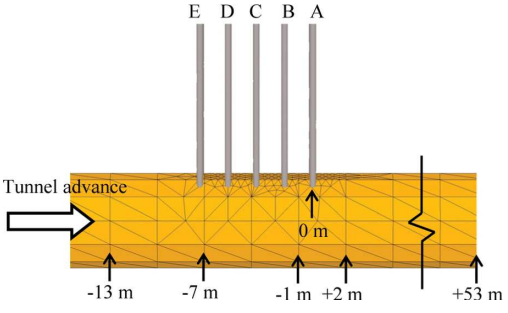

Figure 6. Selected tunnel face positions relative to row A piles.

Figure 7(a) shows the predicted settlements (u_z) of pile A1. At Stage –1 m prior to the pile cutting, the maximum pile u_z is 22 mm and the settlement at the pile head is larger than the pile toe. Immediately after the pile cutting (Stage +2 m), the maximum u_z increases to 29 mm and the settlement in the pile mid-section is smaller than the pile head and toe. At Stage +53 m, the final maximum u_z is 38 mm occurring at the pile toe.

Figure 7(b) shows the predicted axial forces (N) of pile A1. Up to Stage –1 m, the pile N increase due to negative skin friction induced by tunnelling. As the pile toe is cut at Stage +2 m, the pile N decrease due to undermining below the cut pile toe and correspondingly mobilisation of positive skin friction. At the final Stage +53 m, a portion of the cut pile toe experiences tensile forces with a maximum of –160 kN. Compared to the initial pile N profile before tunnelling (denoted as Initial), the final pile N has increased in the upper levels from –1.5 to –10 mPD and decreased in the lower levels from –10 to –20.3 mPD.

Figure 8(a) shows the predicted transverse horizontal displacements (u_x) of pile A1. The direction of u_x is perpendicular to the tunnel alignment.

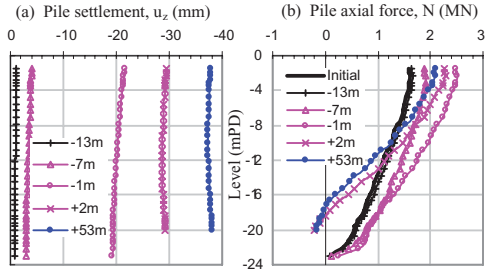

Figure 7. Predicted pile settlements and axial forces of A1.

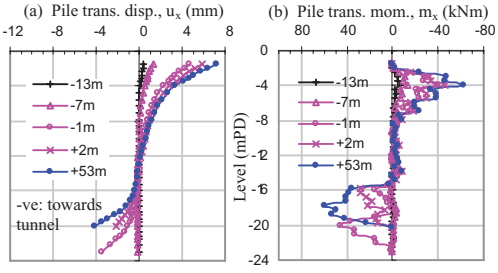

Figure 8. Predicted pile transverse u_x and m_x of A1.

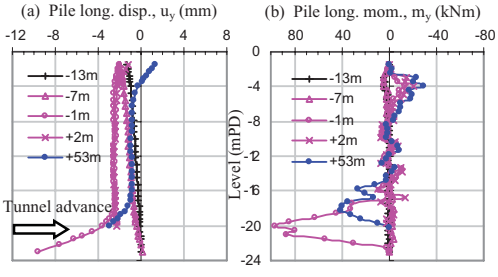

Figure 9. Predicted pile longitudinal u_y and m_y of A1.

The rate of pile u_x increases when the tunnel face approaches (Stage –1 m) and passes (Stage +2 m) pile A1. The final maximum pile u_x is 7 mm. The pile head u_x show positive values following the direction of pile cap/building horizontal displacements, whereas the pile toe u_x show negative values towards the tunnel centreline. Figure 8(b) shows the predicted transverse bending moments (m_x) of pile A1. A maximum pile m_x of 60 kNm is predicted at the –18 m PD level.

Figure 9(a) shows the predicted longitudinal horizontal displacements (u_y) of pile A1. The direction of u_y is parallel to the tunnel alignment. At Stage –1 m immediately prior to the pile-cutting, the pile toe shows a drastic increase in u_y to 10 mm towards the tunnel face, which is a transient value as the pile toe is cut off later. At Stage +53 m,

the final maximum u_y at the cut pile toe is 3 mm. Figure 9(b) shows the predicted longitudinal bending moment (m_y) of pile A1. A maximum m_y of 96 kNm is predicted at the –20 mPD level at Stage –1 m, which is a transient value. At Stage +53 m, the final m_y is 41 kNm occurring at the -18 mPD level. It is noted that the final pile horizontal displacement and bending moment are more critical in the transverse direction (final max. u_x = +7 mm, m_x = 60 kNm) than in the longitudinal direction (final max. u_y = –3 mm, m_y = 41 kNm).

Figure 10(a) shows the predicted settlements (u_z) of pile A5 located a horizontal distance of 2.4 m from the tunnel springline (see Figure 1). At Stage +53 m, the final maximum u_z is 25 mm. The pile head settlement is slightly larger than the pile toe settlement, indicating that negative skin friction is induced on the pile shaft due to tunnelling. Figure 10(b) shows the predicted axial forces (N) of pile A5. The pile N increase due to tunnelling, and the pile head N increases from an initial of 1003 kN to the final of 1191 kN at Stage +53 m.

Figure 11(a) shows the predicted transverse horizontal displacements (u_x) of pile A5. The whole pile has displaced horizontally towards the tunnel with a final maximum of 7 mm at the pile head. Figure 11(b) shows the predicted transverse bending moments (m_x) of pile A5. The final maximum m_x is 48 kNm occurring at the -18 mPD level.

Figure 12 shows the predicted building settlements (s_z) at the selected tunnelling stages for Analysis 1. The settlements are on the building rear edge. About 65% of the total building settlements occur up to Stage -1 m. The final maximum s_z is 40 mm, and the building settles and tilts as a rigid body.

Figure 13 compares the predicted greenfield ground surface settlement curve with the building settlement curve at Stage +53 m for the baseline Analysis 1. The greenfield curve represents a transverse section far away from the building, the location of which is not affected by the building/pile stiffness. The maximum building settlement of 40 mm is about 7 times larger than the maximum greenfield surface settlement of 6 mm, due to the pile-cutting and undermining below the cut pile toes. GCO (1985) observed the similar behaviour of building settlements being larger than greenfield surface settlements on a tunnelling project which involved cutting of pile toes located at the tunnel axis level. Lee et al. (2010) and Lee et al. (2011) also predicted the behaviour of building settlements being larger than greenfield surface settlements in 3D FEA analysing a building supported by a group of friction piles with the pile toe levels corresponding to the tunnel crown level.

Results for the parametric study Analyses 2 and 3 are compared to the baseline Analysis 1 in terms

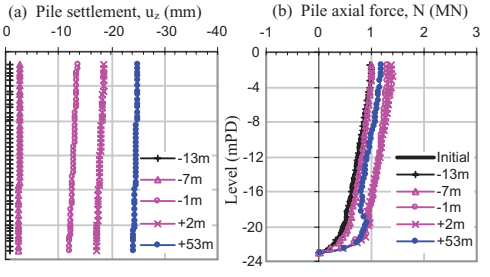

Figure 10. Predicted pile settlements and axial forces of A5.

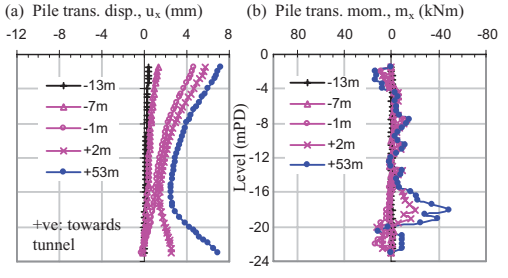

Figure 11. Predicted pile transverse u_x and m_x of A5.

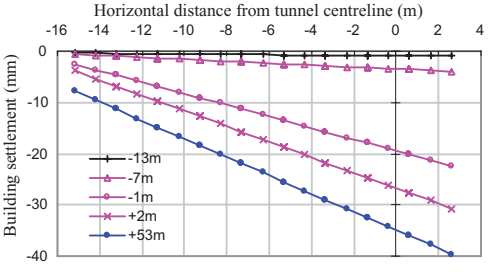

Figure 12. Predicted building settlements for Analysis 1.

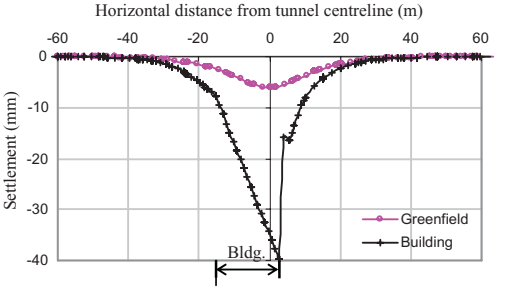

Figure 13. Greenfield & building settlements for Analysis 1.

of the predicted building settlements and selected responses of pile A1. Figure 14 compares the predicted final building settlements (s_z) at Stage +53 m between the three analyses. Analysis 2 modelling the upper half of a 3 m thick grouted annulus predicts 16 mm, whereas Analysis 3 modelling a full 3 m thick grouted annulus predicts the least maximum building settlement of 11 mm. This result suggests that if the grouting work is carried out close to the source of ground movements immediately around/in the tunnel area, the movement of the piles/building can be significantly reduced by 60% to 73%. To reduce further the building settlement, the thickness and length of the grouted annulus have to be increased.

Figure 15(a) compares the predicted settlements (u_z) of pile A1 at Stage +53 m between the three analyses. The half and full grouted annulus schemes reduce the maximum pile u_z from 38 mm (no grouting) to 15 mm and 11 mm respectively. Figure 15(b) compares the predicted axial forces (N) of pile A1 at Stage +53 m between the three analyses. Both grouting schemes predict compressive N throughout the pile length. This demonstrates the effectiveness of the grouted annulus schemes in reducing pile settlements and preventing the cut pile toe from experiencing tensile forces.

The predicted final pile N and m_x of pile A1 from the three parametric study analyses are checked against the pile axial force-moment (N-M) interaction chart of structural capacity, see Figure 16. Analyis 3 with a full 3 m thick grouted annulus has a higher margin of safety against exceeding the pile capacity envelope, followed by Analysis 2 with the upper half of a 3 m thick grouted annulus and Analysis 1 without grouting.

Figure 17 shows the predicted final building horizontal displacements and horizontal strains for Analysis 1. The maximum tensile horizontal strain (ε_h) is 1.7×10^{-4}%. The results from Analyses 2 and 3 are not presented because they are smaller than Analysis 1.

A check on the risk of building damage is carried out using Burland's (1995) assessment chart based on buildings deflection ratio (Δ/L) and ε_h. Please note that parameter Δ is relative deflection and L is length over the relative deflection range. For Analysis 1 the predicted maximum Δ/L is 7.1×10^{-4}% and maximum $_h$ is 1.7×10^{4}%. Figure 18 shows that the predicted category of risk of building damage is Category 0 (or Negligible) due to consideration of the building superstructure rigidity.

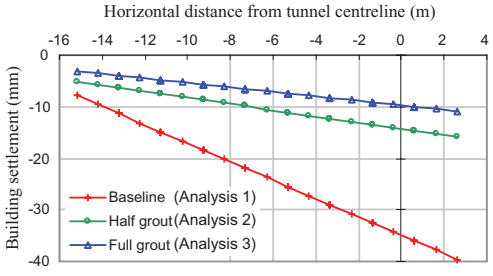

Figure 14. Building settlements for parametric analyses.

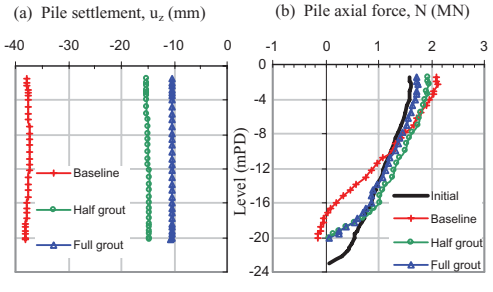

Figure 15. Results of parametric analyses for pile A1.

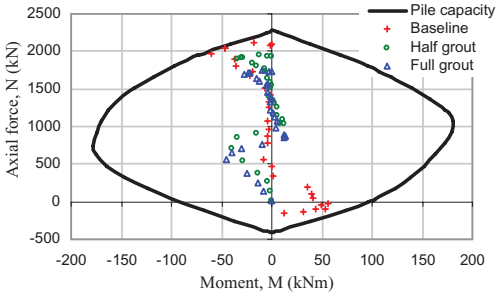

Figure 16. N-m_x of pile A1 vs. pile N-M interaction chart.

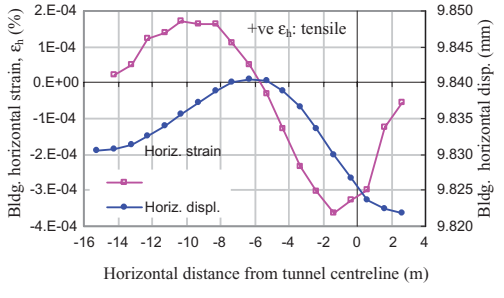

Figure 17. Building horizontal displacements and strains.

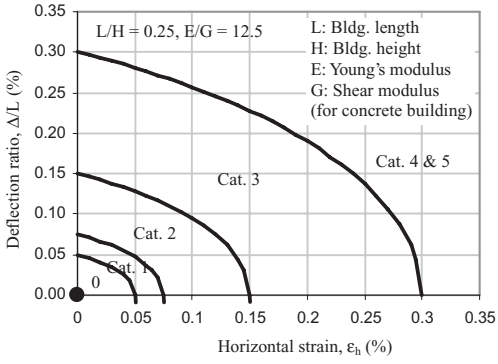

Figure 18. Burland's building assessment chart.

5 CONCLUSION

3D FEA have been carried out to model construction of a 6 m diameter bored tunnel intersecting the lower portion of a large pile group comprising 50 nos. of 0.6 m diameter friction piles supporting a high-rise building. The pile toe levels correspond to the tunnel axis level and 15 nos. of the obstructing pile toes are cut off as the tunnel passes through. A step-by-step pressure method is used to model the progressive advance of tunnelling with an overpressure of 20 kPa (i.e. the confinement pressure hydrostatic pore water pressure 20 kPa).

The most critical corner pile subjected to pile-cutting is predicted to settle by 38 mm. The pile axial force is reduced due to undermining below the cut pile toe, and a portion of the pile toe experiences tensile forces. The predicted final pile horizontal displacement (u) and bending moment (m) are more critical in the transverse direction (final max. u_x 7 mm, m_x 60 kNm) than in the longitudinal direction (final max. u_y -3 mm, m_y 41 kNm). An edge pile located at a horizontal distance of 2.4 m from the tunnel springline is predicted to settle by 25 mm and the pile axial force is increased due to the negative skin friction induced by tunnelling. The predicted maximum building settlement is larger than the maximum greenfield surface settlement by about 7 times without any protective measure.

Protective measures in the forms of the upper half of and a full 3 m thick grouted annulus around the tunnel are predicted to reduce the maximum building settlement from 40 mm (no grouting) to 16 mm and 11 mm respectively. Both grouting schemes can prevent the most critical cut pile from experiencing tensile forces near the toe. This result suggests that grouting work carried out close to the source of ground movements around/in the tunnel area is effective in mitigating tunnelling-induced ground movements.

The predicted pile axial forces (N) and bending moments (M) of the most critical pile are compared to the pile N-M interaction chart of structural capacity to check for potential over-stressing of the pile structurally. The predicted maximum building deflection ratio and horizontal tensile strain are plotted on Burland's assessment chart to determine the category of risk of building damage.

The numerical work presented in this paper has demonstrated the merits of using 3D FEA in analysing tunnel-soil-pile-building interaction problems in a rigorous manner. With advances in computing technologies, 3D FEA of practical geotechnical problems is now possible complementing conventional methods of analysis.

REFERENCES

Benz, T., Vermeer, P.A. & Schwab, R. 2009. A small-strain overlay model. *Int. J. Numer. Anal. Meth. Geomech*. 33: 25–44.

Burland, J.B. 1995. Assessment of risk of damage to buildings due to tunnelling and excavations. *Invited Lecture to IS-Tokyo'95, Int. Conf. on Earthquake Geotechnical Engineering*.

Engin, H.K., Septanika, E.G. & Brinkgreve, R.B.J. 2008. Estimation of pile group behaviour using embedded piles. *Proc. Int. Conf. 12th Int. Assoc. Comp. Methods Advances Geomech., Goa, India*: 3231–3238.

GCO 1985. MTR Island Line: Effects of construction on adjacent property. Geotechnical Control Office, Engineering Development Department, Hong Kong.

Lee, S.W., Choy, C.K.M., Cheang, W.W.L., Swolfs, W. & Brinkgreve, R. 2010. Modelling of tunnelling beneath a building supported by frictional bored piles. *Proc. of 17th Southeast Asian Geotechnical Conference, Taipei, May*: 215–218.

Lee, S.W., Choy, C.K.M., Tse, S.C., van Gool, F.R., Cheang, W.W.L. & Brinkgreve, R.B.J. 2011. Modelling of tunnelling near a building supported by large numbers of piles. *Proc. of 14th Asian Regional Conf. on Soil Mech. & Geot. Engrg., Hong Kong, May*: in press.

Lee, S.W., Pickles, A.R., Henderson, T.O., Li, E.S.F. & Cheang, W.W.L. 2008. 3D modelling of deep excavation in decomposed granite: influence of small strain stiffness and presence of individual piles. *Proc. of Applications on Innovative Technologies in Geotechnical Works, HKIE, Geot. Div. 28th Annual Seminar*: 171–180.

Ng, C.W.W., Pun, W.K. & Pang, R.P.L. 2000. Small strain stiffness of natural granitic saprolite in Hong Kong. *J. Geotech. & Geoenv. Engrg., ASCE* 126(9): 819–833.

Pang C.H. 2006. The effects of tunnel construction on nearby pile foundation. PhD thesis, National University of Singapore.

Plaxis 2010. Plaxis 3D Reference Manual, Version 2010, Release Candidate 1.

Potts, D.M. & Addenbrooke, T.I. 1997. A structure's influence on tunnelling-induced ground movements. *Geotechnical Engineering Proc. ICE* 125: 109–125.